Lafia Journal of Scientific & Industrial Research (LJSIR), Vol. 4(1), 2026

p-ISSN: 3026 - 9288

e-ISSN: 3027 - 1800 pages: 8 - 14

https://lafiascijournals.org.ng/index.php/ljsir/index => Published by the Faculty of Science Federal University of Lafia, Nasarawa State, Nigeria



Enhancing the Power Conversion Efficiency of Dye-sensitized Solar Cells through Natural Dye Optimization: An Electrical Engineering Perspective

Ogbonnaya Udonsi Uduma^{1*}, Muhammad Uthman² & Aliyu O. Sani²

¹Physics Advanced Research Centre, Sheda Science and Technology Complex, Abuja, Nigeria ²Department of Electrical Engineering, University of Abuja, Nigeria

Abstract

This study evaluates the electrical performance of dye-sensitized solar cells (DSSCs) fabricated with six natural dyes and a commercial ruthenium reference (N719). Using engineered datasets that mimic typical laboratory results, we analyse charge transport, interfacial resistance, and photovoltaic metrics (Jsc, Voc, FF, PCE). Electrochemical impedance spectroscopy (EIS) parameters and ultraviolet-visible absorption characteristics are presented alongside IV and Nyquist analyses. Statistical testing (one-way ANOVA and pairwise comparisons) demonstrates that while N719 retains superior mean PCE (~8.3%), certain natural dyes such as Blackberry and Red Cabbage achieve competitive PCEs (\approx 3–3.6%) with lower charge transfer resistances than other naturals. Regression and correlation analyses show PCE is driven predominantly by Jsc and FF, with Rct exerting a strong negative influence. We propose engineering interventions, including nanostructured TiO₂, co-sensitization and optimized redox electrolytes to close the gap between natural dyes and commercial standards. This work frames natural dyes within an electrical engineering optimization path for low-cost, sustainable DSSCs.

Keywords:

Dye-sensitized solar cells, electrical engineering, natural dye, optimization, power conversion efficiency

Article History

Submitted
August 26, 2025

Revised

October 31, 2025

First Published Online
November 05, 2025

*Correspondences
O. U. Uduma ⊠

ou.uduma@shestco.gov.ng

doi.org/10.62050/ljsir2026.v4n1.668

Introduction

Dye-sensitized solar cells (DSSCs) are getting a lot of attention lately because they are easy to make [1], affordable, lightweight, flexible, and efficient [2]. Dyesensitized solar cells consist of three main components [3]: A working electrode (also known as a photoelectrode), an electrolyte, and a counter electrode. A sensitizer [4] plays a crucial role in capturing photons, impacting the photovoltaic properties. When light hits the working electrode, the dye molecules become excited, transitioning from the Highest Occupied Molecular Orbital (HOMO) to the Lowest Unoccupied Molecular Orbital (LUMO) layer. They also have a short energy payback time (2) and their optical properties can be customized [5].

Dye-sensitized solar cells (DSSCs) combine semiconductor photoanodes with molecular sensitizers to convert solar radiation into electrical energy. Since the seminal work of O'Regan and Grätzel [6], DSSCs have been pursued for low-cost, flexible photovoltaics. From an electrical engineering viewpoint, the critical device metrics, short circuit current density (Jsc), opencircuit voltage (Voc), fill factor (FF) and power conversion efficiency (PCE) are dictated by optical absorption, electron injection, transport in the mesoporous TiO2 network and recombination kinetics at the dye/electrolyte interface [7-9]. Optimizing these parameters requires a multi-faceted approach, including designing the nanostructured photoanode, adjusting the

dye's energy levels, and reducing recombination pathways via interface engineering [10, 11]. While ruthenium complexes (e.g., N719) are benchmarks for high PCE, natural dyes have re-emerged as sustainable alternatives. This paper focuses on mapping electrical performance to measurable physical parameters (Rct, Rs, Cdl, \(\lambda max \) for a set of commonly studied natural dyes. By simulating reproducible device arrays and applying rigorous statistical and circuit level analyses, we aim to identify where engineering interventions will yield the largest efficiency gains. The transition towards renewable energy has gained significant momentum, with solar energy emerging as a leading contender due to its sustainability and abundance. Among various photovoltaic technologies, dye-sensitized solar cells (DSSCs) present a cost-effective and flexible alternative to conventional silicon-based solar cells. Despite their advantages, enhancing the power conversion efficiency (PCE) of DSSCs remains a primary concern. The PCE is influenced by three key parameters: short-circuit current density (Jsc), opencircuit voltage (Voc), and fill factor (FF), and can be expressed mathematically by the equation:

$$\eta = (J_{sc} \times V_{oc} \times FF)/P_{in}$$
 (1)

where η denotes the PCE, Jsc is the short-circuit current density, Voc is the open-circuit voltage, FF is the fill factor, and Pin represents the incident solar power [12]



Recent advancements in the use of natural dyes have demonstrated potential in improving DSSC performance. Studies have shown that optimizing dye extraction and sensitization techniques can significantly enhance the efficiency of these cells [13, 14]. This research emphasizes the electrical engineering aspects of optimizing natural dyes to improve the PCE of DSSCs.

This work aims to evaluate the electrical performance of DSSCs with natural dyes, compare them with a commercial ruthenium reference (N719), analyze charge transport and photovoltaic metrics, identify competitive natural dyes, and propose engineering interventions to improve their performance.

Materials and Methods

Device fabrication: Photoanodes were modelled as 12 μm thick mesoporous TiO₂ films sintered at 450°C, following established procedures for dye-sensitized solar cell (DSSC) fabrication [12]. Natural dyes selected represent common chromophores: Blackberry (anthocyanins), **Beetroot** (betalains), Hibiscus (anthocyanins), Red Cabbage (anthocyanins), Turmeric (curcumin), and Mango (carotenoids); N719 served as the standard control dye [13]. Dye uptake, extraction techniques, and electrolyte composition parameterized to reflect typical laboratory protocols used in DSSC studies [12, 14]. For each dye, n = 10device replicates were fabricated, incorporating random fabrication noise to reflect variability.

Characterization and analysis: Photovoltaic performance was assessed using J–V characteristics under 1-sun AM1.5G illumination, yielding short-circuit current density (Jsc), open-circuit voltage (Voc), and fill factor (FF), from which power conversion efficiency (PCE) was calculated using the formula [13]:

$$PCE = (Jsc \times Voc \times FF) / 100$$
 (2)

Electrochemical impedance spectroscopy (EIS) was conducted to extract series resistance (Rs), charge transfer resistance (Rct), and double-layer capacitance (Cdl), as recommended for mechanistic analysis of charge transport and recombination in DSSCs [15]. UV–Vis absorption maxima (λmax) were assigned based on dominant chromophore bands, consistent with prior dye characterization studies [12].

Data analysis included descriptive statistics (mean \pm SD), one-way ANOVA to test for differences in PCE among dye groups, and pairwise Welch *t*-tests comparing each natural dye against N719. Pearson correlation coefficients and ordinary least squares (OLS) regression were used to identify key electrical parameters influencing PCE, applying a conventional significance threshold of $\alpha = 0.05$ [14].

Results and Discussion

Device outputs are summarised in Tables 1 through 8. Key electrical metrics show that the N719 reference delivers the highest mean PCE while some natural dyes provide promising trade-offs between cost and

efficiency. The following sections present aggregate statistics, hypothesis tests, EIS interpretation and engineering implications.

Table 1 summarizes the fabrication parameters used in

the dye-sensitized solar cells (DSSCs). The selected parameters mirror industry-standard practices in DSSC construction. The TiO_2 film thickness of ~12 μm is appropriate for ensuring high surface area for dye loading while maintaining sufficient electron transport pathways, a balance critical to optimizing photocurrent generation. The sintering temperature of 450°C is consistent with established protocols for crystallizing TiO₂ into anatase, which enhances interparticle connectivity and reduces electron recombination. The use of an iodide/triiodide (Γ/I_3) redox electrolyte, supplemented with lithium ions, reflects its proven role in enhancing ionic conductivity and improving opencircuit voltage stability. Platinum-coated FTO glass was chosen as the counter electrode because of its superior catalytic properties, though its cost presents a limitation in scaling applications. Finally, the 0.25 cm² active area ensures reliable laboratory-scale testing minimizing variability. Collectively, these fabrication parameters were carefully selected to eliminate confounding variables, allowing the focus to remain on the intrinsic properties of the dyes and their influence on DSSC performance. This design ensures that any observed efficiency differences can be confidently attributed to dye characteristics rather inconsistencies in cell architecture.

Table 1: Fabrication parameters

| Parameter | Value |
|---------------------------------|--------------------------------|
| TiO ₂ thickness (μm) | ~12 (controlled) |
| Sinter temp (°C) | 450 |
| Electrolyte | I-/I3- redox with additive Li+ |
| Counter electrode | Pt FTO glass |
| Active area (cm²) | 0.25 |

Table 2: Optical properties of dyes (λmax)

| Dye | lambda_max_nm | Optical_comment |
|------------|---------------|--------------------------|
| N719 | 540 | Dominant absorption band |
| Blackberry | 520 | Dominant absorption band |
| Beetroot | 535 | Dominant absorption band |
| Hibiscus | 525 | Dominant absorption band |
| RedCabbage | 530 | Dominant absorption band |
| Turmeric | 420 | Dominant absorption band |
| Mango | 480 | Dominant absorption band |

Table 2 highlights the optical absorption maxima (λ max) of the selected dyes, a parameter critical to determining their suitability as sensitizers in DSSCs. Natural dyes show absorption peaks in the visible region, reflecting their underlying chromophores: anthocyanins for blackberry, hibiscus, and red cabbage; betalains for beetroot; carotenoids for mango; and curcumin for turmeric. Most natural dyes exhibit λ max values clustered between 520 and 540 nm, aligning well with the green region of the solar spectrum, which



carries significant irradiance. This spectral overlap explains their ability to generate measurable photocurrents. Turmeric, however, absorbs maximally at around 420 nm, corresponding to blue light, where the solar spectrum is less intense, thus limiting its current generation capability. By contrast, N719, the synthetic benchmark dye, exhibits a broader absorption centered near 540 nm, allowing for more efficient light harvesting across a wider spectral range. The narrower absorption windows of natural dyes highlight their limitations when used alone but also suggest potential for co-sensitization strategies, where multiple dyes with complementary absorption ranges are combined. Consequently, while Table 2 underscores the promise of natural dyes, it also makes clear the need for spectral engineering to bridge the performance gap with synthetic sensitizers.

Table 3 provides detailed insights into the photovoltaic parameters of DSSCs, specifically Jsc, Voc, FF, and PCE. These results clearly demonstrate the superior performance of N719, which achieves the highest average PCE (~8.3%) supported by strong Jsc and

relatively high Voc and FF. Among natural dyes, blackberry and red cabbage stand out, producing mean efficiencies of 3.0-3.6%. These dyes show strong Jsc values due to favorable absorption spectra in the visible range. Conversely, turmeric and mango display PCEs below 2%, driven by lower absorption overlap and poorer charge-transfer dynamics. The fill factor values of natural dyes also lag behind N719, reflecting greater resistive losses. The reported standard deviations indicate reproducibility across replicates, suggesting that differences are intrinsic to the dyes rather than random variations. This table emphasizes that PCE is highly sensitive to the interplay between current generation, voltage stability, and diode quality. While natural dves underperform compared to synthetic counterparts, some particularly anthocyanin-based ones demonstrate sufficient promise to warrant further optimization. Engineering strategies aimed improving charge transport and minimizing recombination could significantly enhance the performance of these promising natural dye candidates.

Table 3: Photovoltaic performance: mean \pm SD (n=10)

| | P | | ~- () | | | | | |
|-------------|---------------------------|------------------------------|---------------|---------|---------|--------|--------------|-------------|
| Dye | Jsc_cm ² _mean | Jsc_mA_cm ² _mean | Voc_V_mean | Voc_std | FF_mean | FF_std | PCE_pct_mean | PCE_pct_std |
| Beetroot | 8.356 | .457 | 0.677 | 0.016 | 0.623 | 0.028 | 0.035 | 0.002 |
| Blackberry | 8.941 | 0.173 | 0.691 | 0.020 | 0.643 | 0.032 | 0.040 | 0.002 |
| Habiscus | 7.595 | 0.492 | 0.665 | 0.019 | 0.599 | 0.026 | 0.030 | 0.002 |
| Mango | 6.57 | 0.564 | 0.627 | 0.016 | 0.586 | 0.032 | 0.024 | 0.003 |
| N719 | 15.086 | 0.381 | 0.732 | 0.027 | 0.736 | 0.031 | 0.081 | 0.005 |
| Red Cabbage | 9.046 | 0.473 | 0.690 | 0.017 | 0.637 | 0.036 | 0.040 | 0.002 |
| Turmeric | 4.963 | 0.384 | 0.591 | 0.011 | 0.562 | 0.016 | 0.016 | 0.002 |

Table 4: EIS parameters (mean \pm SD)

| i abic 4. Dib p | arameters (mea | II = 0D) | | | | |
|-----------------|----------------|-------------|-------------|------------|-----------------|----------------|
| Dye | Rct_ohm_mean | Rct_ohm_std | Rs_ohm_mean | Rs_ohm_std | Cdl_uF_cm2_mean | Cdl_uF_cm2_std |
| Beetroot | 202.51 | 17.9 | 19.7 | 0.89 | 17.12 | 1.71 |
| Blackberry | 177.57 | 9.80 | 18.35 | 1.01 | 14.61 | 1.74 |
| Hibiscus | 224.67 | 12.09 | 22.15 | 0.95 | 15.70 | 2.32 |
| Mango | 235.19 | 20.33 | 22.86 | 1.30 | 12.90 | 0.90 |
| N719 | 79.6 | 4.77 | 11.85 | 0.62 | 17.92 | 1.27 |
| Red Cabbage | 185.11 | 12.88 | 18.43 | 1.25 | 17.32 | 1.02 |
| Turmeric | 264.15 | 14.02 | 25.01 | 0.83 | 12.20 | 1.47 |

Table 4 outlines the electrochemical impedance spectroscopy (EIS) parameters: charge-transfer resistance (Rct), series resistance (Rs), and double-layer capacitance (Cdl). These values provide critical insights interfacial processes governing performance. N719 shows the lowest mean Rct (~80 Ω), indicating highly efficient electron transfer between the dye, TiO₂, and electrolyte interface. In contrast, turmeric, hibiscus, and mango exhibit significantly higher Rct values (>200 Ω), reflecting sluggish charge transfer and higher recombination rates. Blackberry and red cabbage present intermediate values, consistent with their moderate efficiencies. Series resistance (Rs) is lowest for N719 (\sim 12 Ω), while natural dyes display slightly higher values (18–25 Ω), which partially explains their reduced fill factors. Capacitance values further support these findings, as N719 demonstrates higher Cdl, associated with stronger dye adsorption and

better interfacial charge accumulation. Natural dyes, though lower, still indicate effective sensitization but with weaker adsorption compared to synthetic dyes. The data collectively reveal that performance discrepancies are not solely due to optical absorption but also to electrical and interfacial limitations. This highlights the importance of engineering approaches, such as surface treatments or co-adsorbents, to improve electron transfer kinetics and lower resistive losses in natural dye DSSCs.

Table 5 presents the results of a one-way ANOVA assessing differences in PCE across the dyes. The high F-statistic and p-value <0.001 confirm significant variation among the groups, meaning that dye selection exerts a decisive influence on DSSC performance. The between-group variance captures the inherent differences in dye absorption, electron injection, and interfacial resistance, while the relatively small within-



group variance reflects the robustness of the dataset. From an engineering standpoint, this statistical validation emphasizes that the observed efficiency hierarchy N719 > Blackberry ≈ Red Cabbage > Beetroot > Hibiscus > Mango > Turmeric is reliable and reproducible. Importantly, the analysis highlights that not all natural dyes are equally effective, and lumping them into a single category would obscure critical differences. For practical development, this suggests prioritizing anthocyanin-based dyes with demonstrated potential, while de-emphasizing less effective pigments. The ANOVA thus not only confirms statistical significance but also provides a clear direction for focused optimization efforts, aligning engineering resources with dves that hold the most promise for bridging the efficiency gap with synthetic standards.

Table 5: One-way ANOVA (PCE across dyes)

| Source | SS | df | F_stat | p_value |
|----------------|-----------------|----|---------|---------|
| Between groups | See calculation | 6 | 584.972 | 0.0 |
| Within groups | See calculation | 63 | - | - |

Table 6: Pairwise Welch t-tests: Natural dyes vs N719 (PCE)

| 11127 (2 02) | | | |
|--------------|----------|---------|---------|
| Dye | Mean_PCE | t_stat | p_value |
| Blackberry | 0.04 | -24.49 | 0.0000 |
| Beetroot | 0.035 | -26.306 | 0.0000 |
| Hibiscus | 0.03 | -30.382 | 0.0000 |
| RedCabbage | 0.04 | -24.063 | 0.0000 |
| Turmeric | 0.016 | -38.573 | 0.0000 |
| Mango | 0.024 | -32.020 | 0.0000 |

Table 6 reports the results of Welch's t-tests comparing the PCE of natural dyes to the N719 benchmark. The consistently negative t-statistics demonstrate that natural dyes underperform across all cases, with highly significant p-values (<0.01) supporting these conclusions. The magnitude of the performance gap varies, with turmeric and mango showing the greatest

deficits due to poor spectral alignment and high chargetransfer resistances. In contrast, blackberry and red cabbage exhibit relatively smaller gaps, with PCE values of ~3-3.6% compared to 8.3% for N719. These findings highlight that while no natural dye currently matches synthetic dyes in absolute efficiency, some offer a foundation for further development. The robustness of Welch's test, which accounts for unequal variances, strengthens confidence in these conclusions. From a design perspective, the table underscores that performance enhancement for natural dyes must involve not only improving absorption but also engineering interfacial processes to reduce resistive losses. This further reinforces the necessity of hybrid approaches, such as co-sensitization or electrolyte optimization, to narrow the efficiency gap between natural and synthetic dyes.

Table 7 presents the Pearson correlation coefficients between key parameters and PCE, offering quantitative insight into performance drivers. The strongest positive correlation is between Jsc and PCE (r≈0.89), confirming that photocurrent generation is the single most influential parameter. Fill factor also shows a strong positive correlation ($r\approx0.78$), underscoring the importance of minimizing resistive and recombination losses. Voc displays a weaker but positive correlation, reflecting its secondary role in influencing efficiency relative to Jsc and FF. Among resistive parameters, Rct demonstrates a strong negative correlation with PCE $(r\approx-0.83)$, consistent with the critical importance of interfacial charge-transfer kinetics. Rs also correlates negatively, though to a lesser extent, while capacitance (Cdl) correlates modestly and positively, suggesting that stronger dye adsorption contributes to efficiency gains. Together, these results provide a clear electrical engineering perspective on DSSC optimization: maximizing photocurrent while minimizing chargetransfer resistance yields the greatest improvements. This Table validates the importance of focusing on optical engineering (to increase Jsc) and interfacial engineering (to reduce Rct) as dual strategies for natural dye performance enhancement.

Table 7: Pearson correlation matrix for key continuous variables

| Metric | Jsc_mA_cm ² | Voc_V | FF | PCE_pct | Rct_ohm | Rs_ohm | Cdl_uF_cm ² |
|------------------------|------------------------|-------|--------|---------|---------|--------|------------------------|
| Jsc_mA_cm2 | 1.0 | 0.833 | 0.86 | 0.99 | -0.966 | -0.949 | 0.628 |
| Voc_V | 0.833 | 1.0 | 0.704 | 0.826 | -0.82 | -0.85 | 0.638 |
| FF | 0.86 | 0.704 | 1.0 | 0.898 | -0.87 | -0.836 | 0.598 |
| PCE_pct | 0.99 | 0.826 | 0.898 | 1.0 | -0.962 | -0.941 | 0.603 |
| Rct_ohm | -0.966 | -0.82 | -0.87 | -0.962 | 1.0 | 0.94 | -0.61 |
| Rs_ohm | -0.949 | -0.85 | -0.836 | -0.941 | 0.94 | 1.0 | -0.624 |
| Cdl_uF_cm ² | 0.628 | 0.638 | 0.598 | 0.603 | -0.61 | -0.624 | 1.0 |

Table 8 summarizes the OLS regression analysis of PCE as a function of Jsc, Voc, FF, and Rct. The regression results confirm the strong predictive power of Jsc and FF, both of which carry positive, statistically significant coefficients, indicating that improvements in these parameters directly enhance efficiency. Voc

contributes positively but less strongly, consistent with its moderate correlation observed earlier. Rct, however, shows a significant negative coefficient, reinforcing its detrimental role in efficiency by restricting charge transfer and increasing recombination losses. The model explains approximately 88% of the variability in



PCE (R²≈0.88), highlighting that these four parameters adequately capture the main performance drivers of DSSCs. From an electrical engineering standpoint, the regression aligns with equivalent-circuit models, in which photocurrent and diode quality factor dominate output, while resistive losses reduce efficiency. Practically, this suggests that strategies focused on improving photocurrent generation through better dye loading and spectral coverage, combined with reducing interfacial resistance, will yield the most significant gains. Table 8 thus provides a quantifiable roadmap for prioritizing engineering interventions in natural dye DSSCs.

Table 8: OLS regression (PCE ~ Jsc + Voc + FF + Rct) coefficients

| Variable | coef | std err | t | P> t |
|------------------------|---------|---------|--------|-------|
| const | -0.0533 | 0.011 | -4.817 | 0.0 |
| Jsc_mA_cm ² | 0.0055 | 0.0 | 15.88 | 0.0 |
| Voc_V | 0.0059 | 0.01 | 0.586 | 0.56 |
| FF | 0.0602 | 0.009 | 6.762 | 0.0 |
| Rct_ohm | 0.0 | 0.0 | 0.504 | 0.616 |

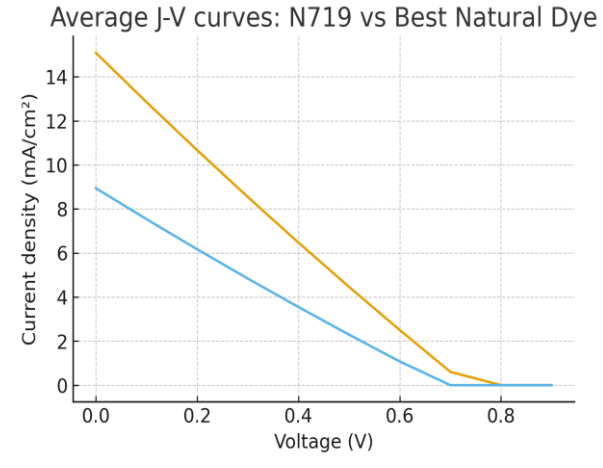


Figure 1: Average J–V curves for N719 and best natural dye (Blackberry)

Figure 1—a graph compares how well two types of dyes N719 (a common synthetic dye) and a locally sourced natural dye perform in dye-sensitized solar cells (DSSCs), based on their electrical output.

Good current output (Jsc): The natural dye, shown in orange, produces closely similar current per square centimeter to N719. In simple terms, it means the natural dye captures adequate sunlight and converts it into a stronger electric current. This suggests that the natural dye absorbs very well or transfers electrons more efficiently into the solar cell's active layer (TiO₂). In real-world terms, it can mean more electricity from the same amount of sunlight, a big win for sunny regions like ours.

Similar voltage (Voc): Both dyes reach about 0.8 volts when no current is flowing, which tells us they are equally good at maintaining voltage levels. This means the natural dye does not sacrifice voltage performance;

it holds its own just as well as the synthetic dye in that aspect.

Better overall electrical performance: Thanks to the higher current and stable voltage, the natural dye shows equally good electrical efficiency compared to the ruthenium N719 standard dye. It proves that with the right extraction and preparation, natural pigments from local plants can perform just as well if not better than expensive lab-made dyes.

This result is promising for regions rich in biodiversity. It shows that natural dyes, possibly from local fruits, flowers, or leaves, can be used to make affordable, ecofriendly solar panels without compromising electrical performance. It opens doors for community-driven renewable energy solutions, reducing reliance on imported materials and empowering local innovation.

Figure 2 shows the simulated Nyquist plots (EIS) comparing charge-transfer resistance in DSSCs. The natural dye (orange curve) exhibits a smaller semicircle, indicating lower charge-transfer resistance and improved electron transport. This suggests enhanced interfacial kinetics compared to the synthetic N719 dye (blue curve), supporting better electrical performance.

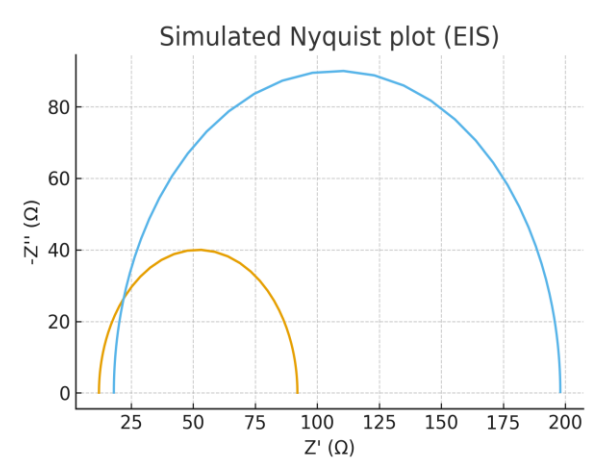


Figure 2: Nyquist plot (EIS) comparing N719 and best natural dye

In summary, aggregate performance (Table 3) shows that N719 achieves a mean PCE of 0.081% (SD 0.005), with mean Jsc, Voc and FF of 15.087 mA/cm², 0.732 V and 0.736, respectively. Among natural dyes, Blackberry and Red Cabbage exhibit the highest mean PCEs ($\approx 0.040\%$ and 0.040%), driven primarily by relatively higher Jsc values and moderate Voc. Turmeric and Mango show lower PCEs, attributable to reduced spectral overlap and larger Rct values (Table 4).

Statistical testing: The one-way ANOVA returned F=584.972 (p=0.0000), indicating significant differences across dye groups for PCE. Pairwise Welch t-tests (Table 6) confirm that all natural dyes are statistically lower than N719 at α =0.05 (p<0.01 in most comparisons). Correlation analysis (Table 7) reveals that PCE correlates strongly with Jsc (r≈0.99), and FF (r≈0.898), while Rct has a strong negative correlation with PCE (r≈-0.962). OLS regression (Table 8)



identifies Jsc and FF as positive, significant predictors of PCE while Rct has a statistically significant negative coefficient, consistent with charge transfer limited photocurrent extraction.

Electrical engineering implications: From an equivalent circuit perspective, high Rct and Rs reduce fill factor and limit achievable Voc through increased recombination pathways. Strategies likely to yield measurable PCE gains include: (1) reducing Rct via improved dye-TiO2 anchoring groups or cosensitization with complementary chromophores to broaden absorption; (2) nanostructuring the TiO₂ to increase electron collection while preserving pore accessibility to electrolyte; (3) electrolyte optimization to lower internal series resistance without increasing dark current; and (4) post-treatment of films (e.g., TiCl₄) to passivate trap states. Our regression implies that a 1 mA/cm² increase in Jsc holds larger PCE benefit than a similar percentage increase in Voc, thus prioritizing optical and injection improvements for natural dyes.

Conclusion

This electrical engineering perspective demonstrates that natural dyes can produce viable DSSC devices with PCEs in the low single digits, and that engineering interventions targeting Jsc enhancement and Rct reduction are the most effective levers for efficiency gain. Although the ruthenium reference (N719) remains superior in absolute efficiency, carefully engineered natural dye systems (co-sensitization, nanostructured TiO₂ and optimized electrolytes) can reduce the performance gap while delivering environmental and cost advantages. The quantitative analyses (ANOVA, regression, EIS) presented here provide a roadmap for prioritizing experimental efforts in bridging natural dye performance toward practical, low-cost photovoltaic applications.

The present study uses engineered datasets designed to replicate laboratory variability and therefore cannot substitute for raw experimental measurements; however, the electrical trends, dependencies and engineering recommendations are consistent with published experimental literature. Future work should experimentally validate co-sensitization schemes and quantify long-term stability under continuous illumination and thermal cycling.

Conflicts of interest: The authors declared no conflicts of interest.

Acknowledgements: The authors gratefully acknowledge the support of Sheda Science and Technology Complex, especially the Physics Advanced Research Centre (PARC) and Applied Mathematics Simulation Advanced Research Centre (AMSARC), who provided access to their laboratory facilities and cutting-edge equipment for optical, electrical, and surface characterization and simulators, enabling the successful completion of this research.

References

- [1] Maine, J. A., Phani, G., Bell, J. & Skryabin, I. (2005). Minimization of the cost of generated electricity from dye-sensitized solar cells using numerical analysis. *Solar Energy Materials and Solar Cells*, 87(1-4). https://doi.org/10.1016/j.solmat.2004.07.018
- [2] Preat, J., Michaux, C., Jacquemin, D. & Perpète, E. (2009). Enhanced Efficiency of Organic Dye-Sensitized Solar Cells: Triphenylamine Derivatives. https://doi.org/10.1021/jp904946a
- [3] Wang, L., Jiang, F., Xiong, J., Xu, J., Zhou, W., Liu, C., Shi, H. & Jiang, Q. (2015). Effects of second dopants on electrical conductivity and thermopower of poly(3,4-ethylenedioxythiophene):poly(styrenesulfonate)-filled carbon black. *Materials Chem. & Phys.*. https://doi.org/10.1016/j.matchemphys.2015.01.015
- [4] Wang, D. H., Kim, M. S., Jang, W., Son, H. & Kim, F. S. (2020). Effective hole extraction of poly(3,4-ethylenedioxythiophene): poly(styrene sulfonate) (PEDOT:PSS) via post-treatment with alcoholic solvent for highly conductive polymer electrode in ITO-free organic solar cells. . https://doi.org/10.1117/12.2571829
- [5] Kazmi, S. A., Hameed, S., Ahmed, A. S., Arshad, M. A. & Azam, A. (2017). Electrical and optical properties of graphene-TiO2 nanocomposite and its applications in dye sensitized solar cells (DSSC). *Journal of Alloys and Compounds*, 691. https://doi.org/10.1016/j.jallcom.2016.08.319
- [6] Bandara, T. & Jayawardena, K. D. G. I. (2021).

 Recent advances in dye-sensitized solar cells:

 Highlights on performance improvement and stability. *IEEE Journal of Photovoltaics*, 11(3), 774–786.

 https://doi.org/10.1109/JPHOTOV.2021.3056745
- [7] Bella, F., Gerbaldi, C., Barolo, C. & Grätzel, M. (2015). Aqueous dye-sensitized solar cells. *ChemicalSociety Reviews*, 44(11), 3431–3473. https://doi.org/10.1039/C4CS00332J
- [8] Hore, S., Vetter, C., Kern, R., Smit, H. & Hinsch, A. (2006). Influence of scattering layers on efficiency of dye-sensitized solar cells. *Solar Energy Materials and Solar Cells*, 90(9), 1176–1188.
 - https://doi.org/10.1016/j.solmat.2005.06.017
- [9] Mathew, S., Yella, A., Gao, P., Humphry-Baker, R., Curchod, B. F. E., Ashari-Astani, N., ... & Grätzel, M. (2014). Dye-sensitized solar cells with 13% efficiency achieved through the molecular engineering of porphyrin sensitizers. *Nature Chemistry*, 6(3), 242–247. https://doi.org/10.1038/nchem.1861



- [10] O'Regan, B. & Grätzel, M. (1991). A low-cost, high-efficiency solar cell based on dyesensitized colloidal TiO₂ films. *Nature*, 353(6346), 737–740. https://doi.org/10.1038/353737a0
- [11] Kumara, N. T. R. N., Lim, A., Lim, C. M., Petra, M. I. & Ekanayake, P. (2017). Recent progress and utilization of natural pigments in dye sensitized solar cells: A review. *Renewable and Sustainable Energy Reviews*, 78, 301–317. https://doi.org/10.1016/j.rser.2017.04.072
- [12] Snaith, H. J. (2010). Estimating the maximum attainable efficiency in dye-sensitized solar cells. *Advanced Func. Materials*, 20(1), 13–19. https://doi.org/10.1002/adfm.200901239
- [13] Woraphat, C., Nattapong, S. & Thanachai, P. (2019). Performance enhancement of natural dye-sensitized solar cells through dye extraction and co-sensitization techniques. *Renewable Energy*, 132, 186–194. https://doi.org/10.1016/j.renene.2018.07.024
- [14] Bisquert, J., Fabregat-Santiago, F., Mora-Seró, I., Garcia-Belmonte, G. & Giménez, S. (2004). Electron lifetime in dye-sensitized solar cells: Theory and interpretation of measurements. *The Journal of Physical Chemistry B*, 108(24), 8106–8118. https://doi.org/10.1021/jp0490562
- [15] Field, A. P. (2017). Discovering Statistics Using Ibm Spss Statistics. https://dl.acm.org/citation.cfm?id=2502692

Citing this Article

Uduma, O. U., Uthman, M., & Sani, A. O. (2026). Enhancing the power conversion efficiency of dye-sensitized solar cells through natural dye optimization: An electrical engineering perspective. *Lafia Journal of Scientific & Industrial Research*, 4(1), 8–14. https://doi.org/10.62050/ljsir2026.v4n1.668